High Yield Synthesis of Cellulose Nanocrystals From Avicel by Mechano-Enzymatic Approach

Laura Spagnuolo, Davide Beneventi, Alain Dufresne, Alessandra Operamolla

ChemistrySelect

Research Article
doi.org/10.1002/slct.202401511

Chemistry Europe
European Chemical Societies Publishing

www.chemistryselect.org

High Yield Synthesis of Cellulose Nanocrystals From Avicel by Mechano-Enzymatic Approach

Laura Spagnuolo,[a, c] Davide Beneventi,[b] Alain Dufresne,[b] and Alessandra Operamolla*[a, c]

Cellulose nanocrystals are an important class of bio-based crystalline nanostructures, finding application in several technological fields, including paper and textile coating, biocomposite engineering, biocatalysts immobilization, etc. This study explores enzymatic hydrolysis of Avicel, using endoglucanase from *Aspergillus niger*, to find an environmentally friendly method to extract cellulose nanocrystals from cellulose sources. Enzymatic hydrolysis has the advantage of reduced energy consumption and higher environmental friendliness compared to acid hydrolysis. In this work, we report for the first time very high nanocrystals yield by combining mechanical pretreatment of the cellulose starting material with a ball miller and endoglucanase hydrolysis, as a result of an extensive optimization of reaction conditions. In particular, a ball milling pretreatment carried out for 50 minutes at 3 Hz, allowed to isolate enzymatic CNCs with 76% yield and with crystallinity as high as 75%. The materials were characterized by X-Ray diffractometry, attenuated total reflectance Fourier transform infrared (ATR-FTIR) spectroscopy, dynamic light scattering, zeta potential and field emission scanning electron microscopy (FE-SEM). Their characteristics were compared with the properties of sulfated CNCs, prepared from Avicel by sulfuric acid hydrolysis. Our results are technologically relevant, as they contribute to the accessibility and sustainability of CNCs for a wide range of applications in various industries.

Introduction

Cellulose, the most abundant natural polymer on Earth, has emerged as a key player in the quest for sustainable materials and technologies.[1] With an increasing focus on green alternatives, the extraction of cellulose nanocrystals (CNCs) from renewable sources,[2–3] such as cellulose-enriched pulps, has garnered significant attention.[4] This study delves into the intricate process of obtaining CNCs from these bioresources.

Cellulose nanocrystals exhibit exceptional mechanical, thermal, and optical properties, making them desirable candidates for various industries, including nanotechnology, biomedicine, composites, and photoactive materials.[5–10] Avicel, a microcrystalline cellulose derived from plant fibers, offers unique opportunities for testing and evaluating CNC extraction procedures. Numerous studies have examined diverse cellulose sources and extraction methods, each offering valuable insights into the field, also pointing at the importance of a green approach.[11,12] However, to navigate the intricacies of this emerging domain, it is imperative to gain a thorough understanding of the extraction process from Avicel while critically evaluating the existing literature. Understanding the nuances of the extraction process on Avicel is crucial for the transfer of know-how to other cellulose-enriched biomasses, not only for advancing the field of nanotechnology but also for addressing the pressing need for sustainable materials.[13]

Controversies within the field center around optimizing extraction methods for specific cellulose sources and assessing their impact on the properties of cellulose nanocrystals (CNCs). Divergent hypotheses regarding the ideal conditions for maximizing yield while preserving nanocrystal integrity underscore the necessity for systematic exploration.[14,15]

Considering the above-described scenario, the objective of this work is to provide in-detail information on the quality of cellulose nanocrystals extracted from Avicel by a combined mechanical-enzymatic approach. Our approach leans towards utilizing greener methods, such as enzymatic hydrolysis in contrast to the acid hydrolysis commonly reported in the literature,[16] to bridge gaps in understanding and provide insights into optimized extraction processes.[17]

For this aim, the selected enzyme is the commercially available endoglucanase from *Aspergillus niger*.[18] Endoglucanase, belonging to the class of cellulases, is an enzyme that plays a crucial role in the cleavage of cellulose. This enzyme is classified in the glycosidic hydrolase family and is responsible for the cleavage of β-1,4-glycosidic bonds within the cellulose chain. The result of this enzymatic activity is the depolymerization of cellulose into smaller oligosaccharides.[19] The use of endoglucanase is particularly significant in various industrial processes, where cellulose degradation is required. Applications

[a] *L. Spagnuolo, A. Operamolla*
Dipartimento di Chimica e Chimica Industriale, Università di Pisa, via Giuseppe Moruzzi 13, I-56124 Pisa, Italy
E-mail: alessandra.operamolla@unipi.it

[b] *D. Beneventi, A. Dufresne*
Université Grenoble Alpes, CNRS, Grenoble INP, LGP2, F-38000 Grenoble, France

[c] *L. Spagnuolo, A. Operamolla*
Interuniversity Consortium of Chemical Reactivity and Catalysis (CIRCC), Via Celso Ulpiani, 27, I-70126 Bari, Italy

Supporting information for this article is available on the WWW under https://doi.org/10.1002/slct.202401511

of endoglucanase[20] include the production of biofuels, specifically the conversion of cellulose into fermentable sugars for the subsequent production of bioethanol from renewable plant biomass;[21] in the textile industry, endoglucanase is used to biopolish cotton fabrics, helping to remove protruding fibers and impurities from the fabric surface and improving the softness and appearance of fabrics;[22] in the pulp and paper industry, endoglucanase plays an important role in pre-bleaching and refining processes, improving the accessibility of pulp to chemicals during bleaching;[23] endoglucanase also finds application in waste treatment processes, where it accelerates the decomposition of cellulose-rich organic materials, such as agricultural residues and municipal solid waste;[24] in the detergent industry, endoglucanase is incorporated into some formulations to improve stain removal from fabrics.[25] In the application of endoglucanase to cellulose depolymerization to CNCs, its effectiveness is determined by the limited accessibility to crystalline domains of cellulose at the standard working enzymatic conditions.[26] Given the preferential selectivity of endoglucanase towards amorphous regions of cellulose, in this work, we combine a mechanical pre-treatment, performed by ball milling,[27] to enzymatic hydrolysis to enhance reaction yields, with the aim of producing mechano-enzymatic CNCs with comparable properties to nanocrystals produced by acid hydrolysis.

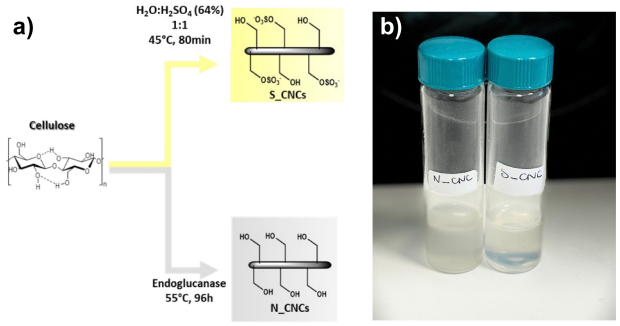

Figure 1. a) Schematic representation of the synthesis of cellulose nanocrystals: comparison between acid hydrolysis and enzymatic hydrolysis; b) photos of aqueous suspensions of S_CNCs and N_CNCs at 5 mg mL^{-1} concentration in water.

Results and Discussion

Preparation of CNCs From Avicel

CNCs were prepared from Avicel by acid and enzymatic hydrolysis, as depicted in Figure 1. Sulfated CNCs (S_CNCs) were prepared as reference materials from Avicel by hydrolysis with 64% sulfuric acid at 45 °C.[5,28,29] This procedure yields S_CNCs with an overall yield of 26% (Table 1, Entry 1). This class of CNCs is considered a benchmark by the scientific and market communities, due to their easy dispersibility in water based on their surface charge. For this reason, S_CNCs are presently available on the market.[30] The elemental analysis reveals the composition and structure of S_CNCs, allowing the determination of the average molecular formula and quantification of sulfated substituents and contained water. The resulting formula $C_6H_9O_5(SO_3)_{0.034} \cdot (H_2O)_{0.84}$ indicates a surface sulfation in S_CNC with a degree of substitution (DS) of ~0.034. The observed pH of 3.94 suggests the presence of $-OSO_3^-H_3O^+$ in the lyophilized sample. (Data available in supporting information)

The cellulase treatment of Avicel requires milder conditions, i.e. 55 °C and pH 5.0, controlled using a phosphate buffer. The reaction, performed with *Aspergillus niger*'s endoglucanase under varying enzyme concentrations yielded less satisfactory results, even applying a prolonged incubation period of up to 96 hours. Changes in enzyme concentration from 0.005% to 10% w/w relative to cellulose content can have a significant impact on the efficiency and kinetics of enzyme hydrolysis. At lower enzyme concentrations, such as 0.005%, the rate of hydrolysis is slower due to limited enzyme-substrate interactions, resulting in incomplete conversion of cellulose. Results suggested that the optimal enzyme concentration for the best performance in enzymatic hydrolysis, leading to the production of cellulose nanocrystals, is 10% w/w (Table 1, Entry 4). We did not further investigate increase in enzyme/cellulose ratio, since a higher enzyme-to-substrate loading would not be economically convenient. Therefore, we explored the use of a mechanical pretreatment in order to optimize the reaction.

Table 1. Effect of Hydrolysis Type and Pretreatment Time on Crystallinity Index and Yield of Cellulose Nanocrystals.

Entry	Sample	Pretreatment time [min][a]	Crystallinity Index [%]	Yield [%]	Elemental Analysis				
					C	H	N	S	O[b]
1	S_CNCs	–	88	26	40.10	6.55	0.00	0.60	52.75
2	Avicel	–	80	–	43.09	6.55	–	–	50.58
3	Avicel post BM[c]	10	79	–	43.09	6.55	–	–	50.58
4	Enzymatic CNCs	–	87	7	41.84	6.16	0.08	0.05	51.87
5	Mechanoenzymatic CNCs	10	79	16	41.86	6.03	0.08	0.06	51.97
6	Mechanoenzymatic CNCs	20	73	39	40.81	6.72	0.58	0.06	51.83
7	Mechanoenzymatic CNCs	50	75	76	42.25	6.69	0.03	0.04	50.99

[a] The pretreatment was performed using a ball miller at 3 Hz frequency. [b] Oxygen was calculated by subtracting from 100 C, H, N, and S. [c] BM = ball milling.

Effects of Pretreatment on Avicel

Given the extremely low yield (7%) of N_CNCs extraction by endoglucanase hydrolysis, a mechanical pre-treatment of Avicel was necessary to improve cellulose accessibility to the enzyme. The pre-treatment was performed with a ball miller in inox jars at 3 Hz. The frequency of 3 Hz, coupled with intermittent pauses, played a pivotal role in the mechanical breakdown of Avicel particles, highlighting the dynamic impact of the ball milling on cellulose fibers. Varying outcomes were observed depending on the duration of the applied pre-treatment. A 10 minute treatment resulted in an increase in nanocrystal yield to 16%. Of particular significance, the ball milling exhibited remarkable efficacy in achieving the maximum yield of 76% when a 50 minute pre-treatment at 3 Hz was applied to Avicel. This condition facilitated the mechanical breakdown and hydration of the Avicel fibers, demonstrating the versatility and utility of the ball miller in the cellulose extraction process. Similarly, other literature reports have shown how engineered cellulose enriched biomass, displaying lower polymerization degree and crystallinity, facilitate the access of endoglucanases and cellobiohydrolases, increasing the yield in hydrolysis products.[31] The controlled frequency and duration of treatment exemplify the precision afforded by the ball mill, offering a tailored approach to opening the fibers and enhancing the accessibility of cellulose within the Avicel matrix. Remarkably, our results outperform yields recently reported by others using a planetary mill on a different cellulose source in dry and wet conditions.[32,33]

In both procedures (acid and enzymatic hydrolysis), centrifugation and subsequent washing steps successfully removed residual reactants and by-products, leaving a suspension enriched with cellulose nanocrystals. Sonication further refined the suspensions and a final centrifugation at 1000 rpm for 10 minutes produced a lyophilizable supernatant.

Elemental analyses were carried out to evaluate the composition of the enzymatic N_CNCs. The oxygen (O) content was calculated as the complementary percentage, with $O = 100-(C+H+N+S)$. This comprehensive elemental evaluation provided information on the molecular composition of the samples, contributing to an in-depth understanding of the eventual presence of residual protein. Remarkably, the nearly negligible nitrogen content observed in the analyses of enzymatic CNCs serves as a pivotal indicator. The minimal presence of nitrogen implies that the enzyme was successfully denatured after the reaction and removed by dialysis purification. This strategic elimination of denatured components through dialysis not only validates the success of the reaction but also enhances the overall quality and purity of the experimental outcome.

Characterization of Cellulose Nanocrystals

The isolated S_CNCs and mechanoenzymatic N_CNCs underwent comprehensive characterization using field emission-scanning electron microscopy (FE-SEM), X-ray diffraction (XRD), and attenuated total reflectance Fourier transform infrared (ATR-FTIR) to elucidate their morphology and crystalline structure.

FE-SEM analyses exhibited well-defined nanocrystals with consistent dimensions, showcasing the successful extraction of cellulose nanocrystals from Avicel as noted in Figure 2. The average length of nanocrystals was calculated with the IMAGE J software from AFM topographies (compare Figure S1) and was found to be 95 ± 10 nm and 92 ± 19 nm for S_CNCs and N_CNCs, respectively, whilst the average diameter was 12 ± 3 nm and 10 ± 2 nm for S_CNCs and N_CNCs, respectively.

Figure 3 shows the XRD patterns acquired to confirm the crystalline nature of N_CNCs obtained from mechanically pre-treated Avicel. For comparison, the same analyses were run on Avicel and S_CNCs. The distinctive peaks corresponding to cellulose I were identified in each sample. The crystallinities of the nanocrystals were comparatively assessed using Segal's method,[34] by using the formula:

$$\textit{Crystallinity index}\ (\%) = 100\ x\ \frac{I_{200} - I_{am}}{I_{200}}$$

where I_{200} represents the maximum intensity of the peak with Miller's indexes 200 (centered between 22.4 and 22.6° in cellulose I), while the intensity of the amorphous peak is calculated at the maximum, which depends on the typology of cellulose and is centered at 18° for cellulose I.

Remarkably, the calculated crystallinity of mechanoenzymatic N_CNCs (73–79%) was found to be closely approaching

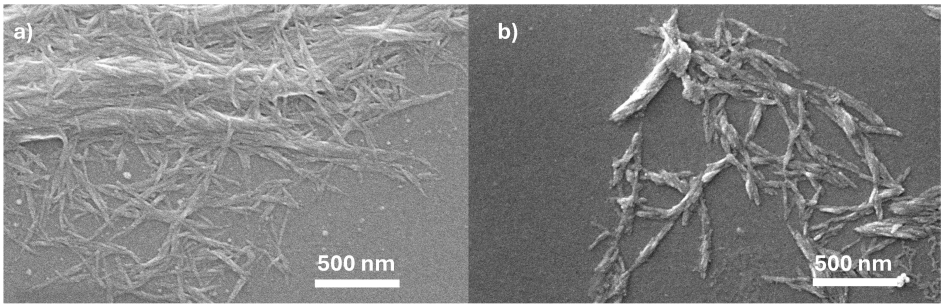

Figure 2. FE-SEM micrographies (120000×magnification) of: a) S_CNC obtained from Avicel by acid hydrolysis with H_2SO_4; (b) N_CNC obtained from Avicel by enzymatic hydrolysis with endoglucanase. Both typologies of nanocrystals were deposited on glass from a 1 mg L^{-1} DMSO suspension.

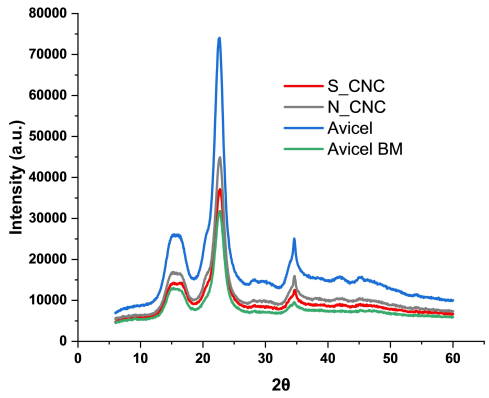

Figure 3. XRD spectra: In blue: Avicel; In green: Avicel Post Ball Mill; In grey: neutral cellulose nanocrystals; In red: sulfated cellulose nanocrystals.

the crystallinity of the starting Avicel material (~80%). Noteworthy, this observation suggests that, despite the prolonged pre-treatment at the ball mill in stainless steel jars, the intrinsic crystalline structure of cellulose I in Avicel was effectively retained after the mechano-enzymatic process. The crystallinity index decrease induced by a dry ball milling process on cellulose structure occurs as an effect of transfers of mechanical energy via ball–ball or ball–vial wall collisions.[35] The minimal changes in crystallinity observed in our experiments underscore the reliability of the extraction method here proposed, emphasizing the possibility of preserving the inherent properties of cellulose even after applying a mechanical pre-treatment.

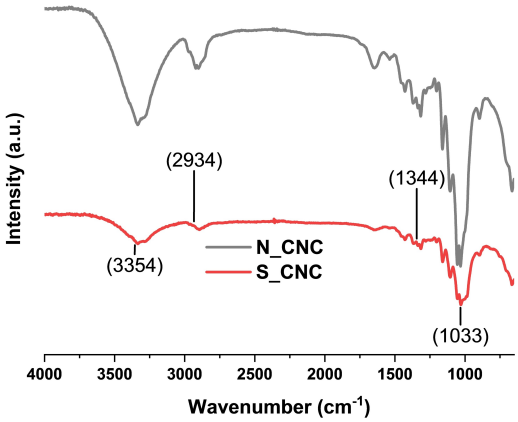

Figure 4. ATR-FTIR spectra: in grey, the spectrum of N_CNC obtained by enzymatic hydrolysis with 50 minutes of pretreatment; in red, the spectrum of S_CNC obtained by sulfuric acid hydrolysis.

In the case of both S_CNCs and N_CNCs, the ATR-FTIR spectra (Figure 4) display the characteristic peaks associated with the various functional groups in cellulose.

One significant feature is the prominent peak observed around 3354 cm^{-1}, corresponding to the stretching vibrations of hydroxyl groups (OH). Another noteworthy region in the spectrum is centered around 2900 cm^{-1}, where signals are attributed to the stretching vibrations of aliphatic carbon-hydrogen bonds of the glycosidic ring (C–H). Furthermore, the intense signals around 1050 cm^{-1} are associated with stretching vibrations of carbon–oxygen bonds (C–O–C). This is prevalent in the glycosidic bonds of cellulose, emphasizing the connectivity of glucose units through the acetal bonds. The small signal centered at 1640 cm^{-1} is attributed to the O–H bending modes of crystallized water contained in the cellulose nanocrystals, as demonstrated by the higher oxygen content found from elemental analyses. In summary, the infrared spectrum of cellulose provides valuable insights into its molecular composition, with distinct peaks corresponding to specific functional groups, pointing at very pure cellulose materials as supported by the elemental analyses, shown in Table 1.

DLS Measurements and Zeta Potential

The results of DLS and zeta potential measurements performed on N_CNCs and S_CNCs water dispersions are shown as histograms in Figure 5 and summarized in Table 2. N_CNCs displayed a relatively narrow size distribution (Figure 5), as indicated by the low polydispersity index (PDI) of 0.4, reported in Table 2. The measured Z-average size was 124 ± 25 nm, in good agreement with the length value found from the FE-SEM micrograph. This suggests that the enzymatic CNCs exhibit a relatively uniform and well-defined size profile, contributing to their homogeneity in the dispersion. S_CNCs displayed a higher polydispersity index (PDI) of 0.5, with a Z-average size of 60 ±

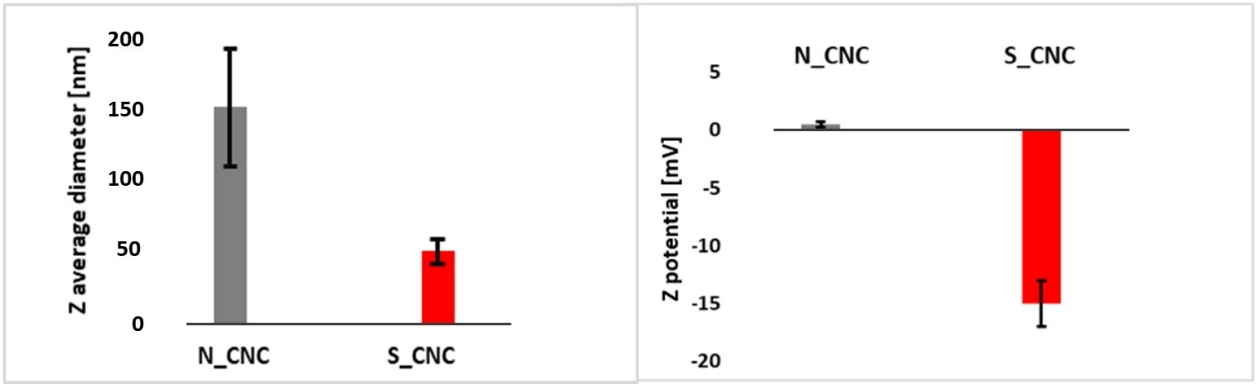

Figure 5. Histograms of DLS (left) and Zeta potential (right) measurements: in grey, N_CNCs; in red, S_CNCs; the scale bars indicate the standard deviation.

Table 2. Characterization of CNC Samples: Polydispersity Index, Z-Average, and Zeta Potential.

Samples	Polydispersity index (PDI)	Z-Average [nm]	Zeta potential [mv]
N_CNC	0.4	150 ± 25	0.5 ± 0.1
S_CNC	0.5	60 ± 8	-15 ± 4

8 nm. The sulfuric acid hydrolysis produces more polydisperse nanocrystals, as an effect of the harsher reaction conditions. Conversely, the high selectivity of the enzymatic treatment is far more reliable in yielding nanocrystals with reproducible features. Despite the higher polydispersity of S_CNCs, their Z-average of 60 nm suggests that the sulfated CNC dispersions are more stable, and this kind of nanocrystals do not separate quickly from water.

The zeta potential histogram (Figure 5, right) of the enzymatic N_CNCs reveals a slightly positive zeta potential of 0.5 ± 0.1 mV, as reported in Table 2, close to neutrality. This low positive charge indicates a negligible repulsion between the neutral N_CNC particles, making them prone to proximity and potential aggregation. The low value of zeta potential suggests that the stability of neutral CNC dispersion may be influenced by van der Waals forces rather than electrostatic repulsion. In contrast, the plot of S_CNC shows a negative zeta potential of -15 ± 4 mV. The negative value indicates greater electrostatic repulsion between the sulfated CNC particles, favoring dispersion stability and confirming what was noted from the DLS measurement. The sulfate groups on the S_CNC surface contribute to the negative zeta potential, preventing agglomeration and improving the overall colloidal stability of the dispersion. The higher negative charge suggests that sulfated S_CNCs are more repulsive, reducing the probability of particle aggregation compared to neutral S_CNCs.

Conclusions

The results demonstrate the successful extraction of CNCs from Avicel utilizing *Aspergillus niger* endoglucanase hydrolysis combined to ball milling pretreatment. The duration of the Avicel pretreatment is recognized as a pivotal factor influencing the yield in CNCs. The characterization has shown a good comparison of N_CNCs properties concerning the benchmarking sulfated CNCs, prepared by sulfuric acid hydrolysis from the same source. Mechano-enzymatic hydrolysis outperforms the acid treatment in terms of reaction yield, with potential economic benefits in the production of these materials. Furthermore, N_CNCs do not entail environmental issues for the waste produced during their preparation as the S_CNCs. Even if the colloidal stability of N_CNC is lower than that of S_CNC, N_CNC suspensions were suitable for DLS and zeta potential measurements, showing that their manipulation may be improved in the right dispersion medium. N_CNCs are more monodisperse, as judged from DLS, demonstrating the higher reliability of the enzymatic approach in producing homogeneous materials. In conclusion, the experimental results demonstrate the feasibility of obtaining cellulose nanocrystals from Avicel using enzymatic hydrolysis. The versatile application of ball milling in opening fibers showcases its usefulness in advancing the efficiency and effectiveness of biomass conversion processes.

Experimental Section

Materials

Avicel® PH-101 (~50 μm particle size) from Sigma Aldrich, Na_2HPO_4 from Sigma Aldrich, Na_3PO_4 from Sigma Aldrich, and Cellulase (1,4-(1,3:1,4) -β-D-Glucan 4-glucan-hydrolase) from MP Biomedicals were used in the experiments.

Preparation of Sulfated CNCs with Acid Hydrolysis

This method was reported by Operamolla et al.[25] 250 mL of deionized water was placed into a 1 L Ace reactor equipped with a water condenser and a mechanical stirrer. The flask was then cooled in an ice bath, and 250 mL of concentrated H_2SO_4 was introduced. Following that, 30 g of Avicel PH-101 was added, and the suspension was heated to 50 °C for a duration of 80 minutes. Subsequently, the system was cooled to room temperature, and the mixture was transferred into polypropylene tubes for centrifugation. Centrifugation at 4000 rpm was repeated, replacing the supernatant liquid with fresh deionized water until the pH of the suspension reached approximately 1. The resulting precipitate was then suspended in deionized water using a Dr. Hielscher 400 W tip sonicator. The sonication process involved a pulsed mode, with a power of 60 W, pulsed at 0.6 s intervals for 10 min. The suspension was subsequently dialyzed with distilled water to achieve neutrality, utilizing a cellulose membrane with a molecular weight of 12,400 Da. The resulting suspension was moved into polypropylene tubes and centrifuged at 4000 rpm for 20 minutes. The supernatant suspension was retained, and water was removed under reduced pressure, yielding 26% cellulose nanocrystals with an average length of 151 ± 15 nm.

Preparation of Neutral CNCs with Enzymatic Hydrolysis

A total of 5.04 g of Avicel was combined with 50 mL of 50 mM phosphate buffer at pH = 5.0 and homogenized using a tissue master. Subsequently, *Aspergillus niger* endoglucanase (28 mg, 253 mg, 516 mg, or 1 g) was introduced into the suspension. The reaction mixture was then placed in an orbital shaker at 55 °C for 96 hours, operating at 150 rpm. Following the incubation period, the reaction was transferred to a beaker and heated from 55 °C to 95 °C for 15 minutes to deactivate the enzyme. The resultant mixture underwent centrifugation at 4000 rpm for 10 minutes. This was followed by a washing step with 20 mL of 0.1 M HCl, followed by another round of centrifugation at 4000 rpm for 10 minutes. To remove the HCl, the solution underwent multiple centrifugations with deionized H_2O (20 mL) at 4000 rpm for 10 minutes, discarding the supernatant each time, until neutrality was confirmed with litmus paper. Upon achieving neutral pH, the reaction underwent a 24 hour dialysis period. Subsequently, the suspension underwent sonication with a Dr. Hielscher 400 W tip sonicator with a ower of 40 W, impulses of 0.6 seconds, for 10 minutes. A final centrifugation at 1000 rpm for 10 minutes was conducted, and the supernatant containing nanocrystals was collected and lyophilized.

Pretreatment of Avicel

When applicable, Avicel pretreatment was conducted using a ball miller with horizontal oscillation (BM500, Anton Paar) equipped with two 50 mL stainless steel jars and 1 2.5 cm diameter ball for each jar. Each jar was loaded with 5 g of Avicel. The pretreatment involved a frequency of 3 Hz for the total time indicated in Table 1 without breaks.

Elemental Analyses

Elemental analyses were performed by the use of a Vario Micro Cube CHNOS Elemental Analyzer. The instrument enables quantitative, fully automated analysis of elements C, H, N, S and O by combustion gas analysis. Gases formed during the combustion process are detected using a thermal conductivity detector (TCD). The weighed sample amount is about 5 mg, each measurement is the average of two analyses and the calibration is done with sulfanylamide.

FE-SEM Analyses

The investigation was made with an FEI FEG-Quanta 450 instrument (Field Electron and Ion Company, Hillsboro, OR, USA). Deposition of cellulose nanocrystals was made on glass from a suspension of DMSO at a concentration of 1 mg/L. The samples were spat out with platinum before analysis.

AFM Topographies

Suspensions of approximately 1 mg L^{-1} of nanocrystals were dispersed in water and then deposited on a mica substrate. The substrate loaded with nanoparticles was analyzed in tapping mode with a Nanoscope IIIa microscope from Veeco Instruments. Silicon cantilevers with a typical radius of curvature of 10–15 nm were used to perform the imaging at a frequency of 264–339 kHz. The topographies were elaborated by using the Nanoscope software. The nanocrystals dimensions, including length (L) and width (W), were measured by using Image J 1.53e software, Institute of Health, USA. Over 50 rod-like nanocrystals were statistically analyzed.

ATR-FTIR Spectra

ATR-FTIR spectra were acquired on a Thermo Scientific (mod. Is50) (Thermo Fischer Scientific, Madison, USA), equipped with an attenuated total reflectance (ATR) diamond cell for measurement in the 4000–4900 range. The attenuated total reflectance (ATR) for measurement in the 4000–650 cm^{-1} region. For each sample, 16 scans with a resolution of 4 cm^{-1} were collected. The ATR-FTIR spectra were recorded in triplicate. Spectra were reprocessed using Origin 2024 as the software.

XRD Spectra

The samples were measured in the X'Pert Pro MPD diffractometer from PANalytical company. The reflection mode and conventional geometry (Bragg-Brentano) was used. A copper anode with characteristic Cu Ka radiation with nickel filters was also used to try to monochromatize the X-ray beam. A sample holder with zero radiation was used. A sample holder with a zero background (single crystal of silicon specially cut to not produce a background signal) with a small cavity that we filled with your sample was used. This cavity has a diameter of 16 mm and is 200 μm deep. The entire surface of the samples was not irradiated, only a square (12 mm×8 mm) was irradiated. The samples were spun at 0.25 Hz.

The Segal method is a widely used technique for estimating the crystallinity index of cellulose based on XRD data. It consists of comparing the intensity of crystalline peaks with the total intensity of crystalline and amorphous peaks. The ratio obtained from this comparison provides an estimate of the crystallinity index.

DLS and Z-Potential Measurements

DLS and zeta-potential measurements were conducted using a Zetasizer Nano ZS instrument from Malvern Panalytical. Common 1 cm UV cuvettes were used to prepare DLS samples while cuvettes with two reduced-volume electrodes were used for zeta potential measurements. Spectra were reprocessed using Origin 2024 as the software.

Supporting Information Summary

All the relevant data are included and commented in the main file of this article. Additional data (determination of degree of sulfatation of S_CNCs from elemental analyses, AFM topographies of S_CNCs and N_CNCs deposited on mica, and ATR-FTIR of all samples included in Table 1) are collected and available free of charge in the Supporting Information to this article.

Acknowledgements

This research was funded by the University of Pisa through the project "BIHO 2022-Bando Incentivi di Ateneo Horizon e Oltre" (Prot. n. 0048740/2022). LS acknowledges MUR (Ministero dell'Università e della Ricerca) for the project PON 2014–2020 (D.M. 1061/2021, CUP I59J21017690008) entitled "Conversion of lignocellulosic biomass into cellulose fibers, lignin, and active biomolecules for the preparation of smart and sustainable coating for textiles of natural origin and similar flexible substrates". The authors thank CISUP (Center for Instrument Sharing of the University of Pisa) for the access to the FE-SEM facility. LGP2 is part of the LabEx Tec 21 (Investissements d'Avenir - grant agreement n ANR-11-LABX-0030) and of the PolyNat Carnot Institut (Investissements d'Avenir - grant agreement n ANR-11-CARN-030-01). Open Access publishing facilitated by Università degli Studi di Pisa, as part of the Wiley - CRUI-CARE agreement.

Conflict of Interests

The authors declare no conflict of interest.

Data Availability Statement

The data that support the findings of this study are available in the supplementary material of this article.

Keywords: Cellulose nanocrystals · Ball milling · Biocatalysis · Endoglucanase · Cellulose hydrolysis · Avicel

[1] X. Zhao, X. Zhou, G. Wang, P. Zhou, W. Wang, Z. Song, *Renew. Energy* **2022**, *192*, 313–325.
[2] Sunil Kumar Ramamoorthy, Dan Åkesson, Rathish Rajan, Aravin Prince Periyasamy, Mikael Skrifvars, 14 - Mechanical performance of biofibers and their corresponding composites, Editor(s): Mohammad Jawaid, Mohamed Thariq, Naheed Saba, In Woodhead Publishing Series in Composites Science and Engineering, Mechanical and Physical Testing of Biocomposites, Fibre-Reinforced Composites and Hybrid Composites, Woodhead Publishing, 2019, Pages 259-292, ISBN 9780081022924, https://doi.org/10.1016/B978-0-08-102292-4.00014-X..
[3] S. Saldarriaga-Hernández, C. Velasco-Ayala, P. Leal-Isla Flores, M. de Jesús Rostro-Alanis, R. Parra-Saldivar, H. M. N. Iqbal, D. Carrillo-Nieves, *Int. J. Biol. Macromol.* **2020**, *161*, 1099–1116.
[4] P. Nehra, R. P. Chauhan, *J. Biomater. Sci. Polym. Ed.* **2020**, *32*, 1–39.
[5] A. Operamolla, C. Mazzuca, L. Capodieci, F. Di Benedetto, L. Severini, M. Titubante, A. Martinelli, V. Castelvetro, L. Micheli, *ACS Appl. Mater. Interf.* **2021**, *13*, 44972–44982.
[6] J. Shojaeiarani, D. S. Bajwa, S. Chanda, *Compos. Part C: Open Access* **2021**, *5*, 100164.
[7] L. Spagnuolo, R. D'Orsi, A. Operamolla, *ChemPlusChem* **2022**, *87*, 202200204.
[8] A. Operamolla, *Int. Journ. Photoen.* **2019**, *16*, 3057929.
[9] S. Sawalha, F. Milano, M. R. Guascito, S. Bettini, L. Giotta, A. Operamolla, T. Da Ros, M. Prato, L. Valli, *Carbon* **2020**, *167*, 906–917.
[10] R. D'Orsi, V. C. Canale, R. Cancelliere, O. Hassan Omar, C. Mazzuca, L. Micheli, A. Operamolla, *Eur. J. Org. Chem.* **2023**, *26*, e202201457.
[11] M. Wang, Y. Wang, J. Liu, H. Yu, P. Liu, Y. Yang, D. Sun, H. Kang, Y. Wang, J. Tang, C. Fu, L. Peng, *Green Carbon* **2024**, *29*, 2950–1555.
[12] R. Zhang, H. Gao, Y. Wang, B. He, J. Lu, W. Zhu, L. Peng, Y. Wang, *Bioresour. Technol.* **2023**, *369*, 128315.
[13] E. C. Ramires, J. D. Megiatto, A. Dufresne, E. Frollini, *Matrix. Fibers* **2020**, *8*, 21.
[14] A. Babaei-Ghazvini, B. Vafakish, R. Patel, K. J. Falua, M. J. Dunlop, B. Acharya, *Int. J. Biol. Macromol.* **2024**, *258*, 0141–8130.
[15] H. Kargarzadeh, M. Ioelovich, I. Ahmad, S. Thomas, A. Dufresne, (2017). Methods for Extraction of Nanocellulose from Various Sources. In Handbook of Nanocellulose and Cellulose Nanocomposites (eds H. Kargarzadeh, I. Ahmad, S. Thomas and A. Dufresne). https://doi.org/10.1002/9783527689972.ch1.
[16] A. A. I. Luthfi, J. M. Jahim, S. Harun, J. P. Tan, A. W. Mohammad, *Process Biochem.* **2016**, *51*, 1527–1537.
[17] L. Solhi, V. Guccini, K. Heise, I. Solala, E. Niinivaara, W. Xu, K. Mihhels, M. Kröger, Z. Meng, J. Wohlert, H. Tao, E. D. Cranston, E. Kontturi, *Chem. Rev.* **2023**, *123*, 1925–2015.
[18] Q. H. Xu, Y. P. Wang, M. H. Qin, Y. J. Fu, Z. Q. Li, F. S. Zhang, J. H. Li, *Bioresour. Technol.* **2011**, *102*, 6536–6540.
[19] T. Perrot, M. Pauly, V. Ramírez, *Plants (Basel)* **2022**, *11*, 1119.
[20] M. Nagl, O. Haske-Cornelius, L. Skopek, *Cellulose* **2021**, *28*, 7633–7650.
[21] R. M. Yennamalli, A. J. Rader, A. J. Kenny, et al., *Biotechnol Biofuels* **2013**, *6*, 136.
[22] D. V. Saravanan, N. S. Vasanthi, T. Ramachandran, *Carbohydr. Polym.* **2009**, *76*, 1–7.
[23] S. Yang, B. Yang, C. Duan, D. A. Fuller, X. Wang, S. P. Chowdhury, J. Stavik, H. Zhang, Y. Ni, *Bioresour. Technol.* **2019**, *281*, 440–448.
[24] U. Kumari, R. Singh, T. Ray, S. Rana, P. Saha, K. Malhotra, H. Daniel, *Plant Biotechnol. J.* **2019**, *17*, 1167–1182.
[25] U. Ejaz, M. Sohail, A. Ghanemi, *Biomimetics (Basel), Biomimeics* **2021**, *5*, 6–44.
[26] P. B. Filson, B. E. D. -Andoh, D. Schwegler-Berry, *Green. Chem.* **2009**, *11*, 1808–1814.
[27] Y. H. Sitotaw, N. G. Abaynesh, S. Nunes, T. Gerven, *Biomass Convers. Biorefin.* **2021**, *13*, 15593–15616.
[28] A. Operamolla, S. Casalini, D. Console, L. Capodieci, F. Di Benedetto, G. V. Bianco, F. Babudri, *Soft Matter* **2018**, *14*, 7390–7400.
[29] O. Hassan Omar, R. Giannelli, E. Colaprico, L. Capodieci, F. Babudri, A. Operamolla, *Molecules* **2021**, *19*, 26–5032.
[30] S. H. Osong, S. Norgren, P. Engstrand, *Cellulose* **2016**, *23*, 93–123.
[31] R. Zhang, Z. Hu, Peng, P. Liu, Y. Wang, J. Li, J. Lu, Y. Wang, T. Xia, L. Peng, *Green Chem.* **2023**, *25*, 1096–1106.
[32] Q. Zhang, Z. Lu, C. Su, Z. Feng, H. Wang, J. Yu, W. Su, *Bioresour. Technol.* **2021**, *331125015*, 0960–8524.
[33] M. Aulitto, R. Castaldo, R. Avolio, M. E. Errico, Y.-Q. Xu, G. Gentile, P. Contursi, *Polymers (Basel)* **2023**, *15*, 1115.
[34] L. Segal, J. J. Creely, A. E. Martin Jr, C. M. Conrad, *Text. Res. J.* **1959**, *29*, 786–794.
[35] R. Avolio, I. Bonadies, D. Capitani, M. E. Errico, G. Gentile, M. Avella, *Carbohyd. Polym.* **2012**, *87*, 265–273.

Manuscript received: March 28, 2024